Wolf effect in homogeneous and inhomogeneous media

Avshalom Gamliel and Govind P. Agrawal

The Institute of Optics, University of Rochester, Rochester, New York 14627

Received January 2, 1990; accepted May 13, 1990

We derive expressions for the spectrum of the field produced by planar, secondary Gaussian Schell-model sources after propagation in free-space, homogeneous dispersive media, and graded-index fibers. Our results show, for the first time to our knowledge, the development of correlation-induced spectral changes (the Wolf effect) as a function of the propagation distance from the source plane. An important result of our study is the prediction of the enhancement of the Wolf effect for propagation in media of index of refraction larger than unity. In the case of graded-index fibers having a parabolic index profile, the source spectrum is shown to reproduce periodically at distances at which such fibers image the source.

1. INTRODUCTION

The changes occurring in the spectrum of light emitted from partially coherent sources as a result of propagation have been the subject of numerous recent investigations.[1–16] Wolf first derived the conditions under which the spectrum of light remains invariant on propagation.[6,17,18] Further work included the examination of spectral effects due to spatial correlations in fluctuations of small sources,[7] as well as in primary and secondary sources of various states of coherence.[8–10] The effect of correlation-induced spectral changes, also known as the Wolf effect, has been verified experimentally in acoustics[12] and in several optical experiments.[11,13,16] The significance of this effect is just becoming apparent in diverse fields such as astronomy, communications, and metrology.

Most of the previous work has focused on light propagation in free space or in a rarefied scattering medium. In this paper we examine the changes in the spectrum of the field occurring on propagation through homogeneous and inhomogeneous dispersive media. In particular, we investigate the development of the spectrum as a function of the propagation distance and its dependence on the state of coherence of the source in both homogeneous and inhomogeneous media. The inhomogeneous medium considered here is a graded-index medium whose refractive index varies quadratically in the radial direction.[19] Such a medium is readily available for experiments in the form of so-called Selfoc fibers.

The changes in the coherence properties of light propagating through various types of waveguide have been investigated by many authors.[20–24] In most of the work encountered in the literature, the state of coherence is characterized by the mutual coherence function.[25] This approach is not suitable for the examination of spectral changes. Agrawal *et al.*[20] considered how the cross-spectral density of the incident light changes on propagation in graded-index fibers. We use their analysis to derive a closed-form expression for the spectrum of the field at an arbitrary distance from the source.

The general expression of the field spectrum derived for a graded-index medium in Section 2 can be used to analyze the spectral changes occurring in a dispersive homogeneous medium in the appropriate limit. The latter result reduces to the well-known free-space result[26] in the limit in which the refractive index is set to unity. Our expression is, however, valid for arbitrary propagation distances and allows us to examine how the spectrum evolves from the near-field to the far-field region. We illustrate our results for free-space spectral evolution in Section 3 by using physical parameters that apply in many practical cases. In particular, we show how the spectrum of light can be shifted toward the shorter or longer wavelength, depending on the propagation distance and the state of coherence of the source.

Spectral evolution in homogeneous media is considered in Section 4. Our results indicate that the spectral shift occurring in the far-zone region is considerably enhanced in a homogeneous medium, with the enhancement factor depending on the index of refraction of the medium. Section 5 is dedicated to the case of inhomogeneous media by considering spectral changes in a graded-index fiber. The main results of the paper are summarized in Section 6.

2. PROPAGATION OF THE SPECTRUM IN GRADED-INDEX FIBERS

The propagation of the cross-spectral density of the field in graded-index fibers has been studied by Agrawal *et al.*[20] In this section we summarize that derivation to establish our notation and derive an expression for the field spectrum.

Consider a graded-index fiber with the axis of symmetry along the z axis (Fig. 1). The fiber is characterized by an index of refraction having the parabolic profile

$$\tilde{n}^2(x, y; \omega) = \begin{cases} n^2(\omega)[1 - \alpha^2(\omega)(x^2 + y^2)] & \text{for } x^2 + y^2 \le {R_0}^2 \quad \text{(1a)} \\ n^2(\omega)[1 - \alpha^2(\omega){R_0}^2] & \text{for } x^2 + y^2 > {R_0}^2 \quad \text{(1b)} \end{cases}$$

where R_0 is the core radius, $n(\omega)$ is the index of refraction at the center of the fiber, α is the radial gradient of the index, and $\omega = k_0 c$ (c is the speed of light) is the frequency associated with the free-space wave number k_0.

It is well known that the modes of a parabolic-index fiber are Hermite–Gaussian functions if Eq. (1a) is assumed to be valid for all x and y.[27] If we also make the scalar and the

0740-3232/90/122184-09$02.00

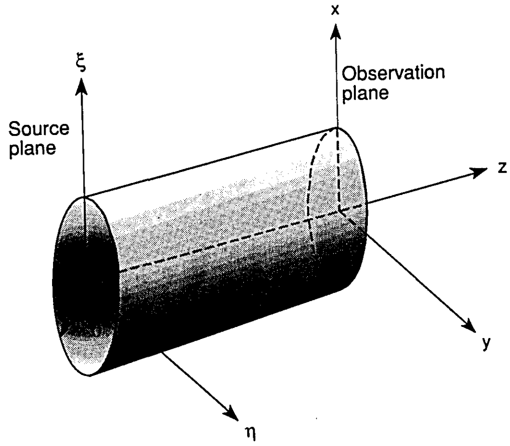

Fig. 1. Illustrating the geometry and the notation. A point in the source plane $z = 0$ is denoted by (ξ, η), and an observation point is denoted by (x, y, z).

paraxial approximations, it can be shown that wave propagation in such a fiber is governed by the formula[20]

$$\Psi(\mathbf{r}; \omega) = \int K(\mathbf{r}, \boldsymbol{\rho}; \omega)\Psi(\boldsymbol{\rho}; \omega)\mathrm{d}^2\rho, \tag{2}$$

where $\Psi(\mathbf{r}; \omega)$ is the optical field and the propagation kernel $K(\mathbf{r}, \boldsymbol{\rho}; \omega)$ is given by

$$K(\mathbf{r}, \boldsymbol{\rho}; \omega) = \frac{k}{2\pi i} e^{i\phi(r)}\left(\frac{\alpha}{\sin \alpha z}\right) \times \exp\left\{\frac{ik\alpha}{\sin \alpha z}\left[\frac{\cos \alpha z}{2}(\xi^2 + \eta^2) - (x\xi + y\eta)\right]\right\}, \tag{3a}$$

$$\phi(r) = k\left[z + \alpha \frac{\cot \alpha z}{2}(x^2 + y^2)\right]. \tag{3b}$$

Here $k = n(\omega)k_0 = n(\omega)\omega/c$, $\boldsymbol{\rho} = (\xi, \eta)$ is a radius vector in the source plane, $\mathbf{r} = (x, y, z)$ is a vector in the direction of observation (Fig. 1), and $n(\omega)$ is the index of refraction at the core center.

The cross-spectral density of the field for any two observation points is given by[20,28]

$$W(\mathbf{r}_1, \mathbf{r}_2; \omega) = \iint K^*(\mathbf{r}_1, \boldsymbol{\rho}_1; \omega)K(\mathbf{r}_2, \boldsymbol{\rho}_2; \omega) \times W(\boldsymbol{\rho}_1, \boldsymbol{\rho}_2; \omega)\mathrm{d}^2\rho_1\mathrm{d}^2\rho_2, \tag{4}$$

where $W(\boldsymbol{\rho}_1, \boldsymbol{\rho}_2; \omega)$ is the cross-spectral density in the plane $z = 0$ and the integration is taken twice over the source domain. The spectrum of the field is obtained by setting $\mathbf{r}_1 = \mathbf{r}_2 = \mathbf{r}$ and is given by

$$S(\mathbf{r}; \omega) = \iint K^*(\mathbf{r}, \boldsymbol{\rho}_1; \omega)K(\mathbf{r}, \boldsymbol{\rho}_2; \omega) W(\boldsymbol{\rho}_1, \boldsymbol{\rho}_2; \omega)\mathrm{d}^2\rho_1\mathrm{d}^2\rho_2. \tag{5}$$

On substituting $K(\mathbf{r}, \boldsymbol{\rho}; \omega)$ from Eq. (3a) into Eq. (5) we obtain the following expression for the spectrum of the field:

$$S(\mathbf{r}; \omega) = \left(\frac{k\alpha}{2\pi \sin \alpha z}\right)^2 \iiiint \mathrm{d}\xi_1\mathrm{d}\xi_2\mathrm{d}\eta_1\mathrm{d}\eta_2 W(\boldsymbol{\rho}_1, \boldsymbol{\rho}_2; \omega) \times \exp\left\{\frac{ik\alpha}{\sin \alpha z}\left[\frac{\cos \alpha z}{2}({\xi_2}^2 - {\xi_1}^2 + {\eta_2}^2 - {\eta_1}^2) - x(\xi_2 - \xi_1) - y(\eta_2 - \eta_1)\right]\right\}. \tag{6}$$

Equation (6) can be used to obtain the field spectrum at the observation point $\mathbf{r}$ for a given form of the cross-spectral density at the source plane $z = 0$. We consider the following specific form of the cross-spectral density of the field in the source plane:

$$W(\boldsymbol{\rho}_1, \boldsymbol{\rho}_2; \omega) = S^{(0)}(\omega)[I(\boldsymbol{\rho}_1)I(\boldsymbol{\rho}_2)]^{1/2}\mu(\boldsymbol{\rho}_2 - \boldsymbol{\rho}_1). \tag{7}$$

Evidently this form implies that the spectrum $S^{(0)}(\omega)$ of the source is the same at all points in the source plane. In the above equation $I(\boldsymbol{\rho})$ is the intensity distribution and $\mu(\boldsymbol{\rho}_2 - \boldsymbol{\rho}_1)$ is the complex degree of spatial coherence. When both $I(\boldsymbol{\rho})$ and $\mu(\boldsymbol{\rho}_2 - \boldsymbol{\rho}_1)$ are taken to be Gaussian functions, the source is known as the secondary Gaussian Schell-model source[29] whose properties have been studied extensively.[30–39] Explicitly, the cross-spectral density of the Gaussian Schell-model source has the form

$$W(\boldsymbol{\rho}_1, \boldsymbol{\rho}_2; \omega) = S^{(0)}(\omega)\exp\left[-\frac{({\xi_1}^2 + {\xi_2}^2) + ({\eta_1}^2 + {\eta_2}^2)}{4{\sigma_I}^2} - \frac{(\xi_2 - \xi_1)^2 + (\eta_2 - \eta_1)^2}{2{\sigma_g}^2}\right], \tag{8}$$

where σ_I is the rms width of the Gaussian intensity distribution (FWHM = 2.35 σ_I) and σ_g is the rms width of the spatial correlation. In general, the quantities σ_I and σ_g depend on frequency. Although their frequency dependence is not shown explicitly, our analysis allows us to incorporate any frequency dependence of σ_I and σ_g.

On substituting Eq. (8) into Eq. (6) and performing the integrations (see Appendix A), we can write the spectrum of the field as

$$S(\mathbf{r}; \omega) = S^{(0)}(\omega)M(\mathbf{r}; k, \alpha; \omega), \tag{9}$$

where the spectral modifier M is given by

$$M(\mathbf{r}; k, \alpha; \omega) = \frac{1}{z^2}\left(\frac{k\sigma_I}{\Delta}\right)^2 \exp\left[-\frac{k^2(x^2 + y^2)/z^2}{2\Delta^2}\right]. \tag{10}$$

Here

$$\Delta = 2ab\sigma_I \frac{\sin \alpha z}{\alpha z}, \tag{11}$$

with the parameters a and b defined by

$$a^2 = \frac{1}{8{\sigma_I}^2} + \frac{1}{2{\sigma_g}^2}, \tag{12}$$

$$b^2 = \frac{1}{2{\sigma_I}^2} + \left(\frac{k\alpha \cos \alpha z}{2a \sin \alpha z}\right)^2. \tag{13}$$

Equations (9) and (10) are the general expressions, valid within the paraxial approximation, for the spectrum of the field produced by planar secondary Gaussian Schell-model sources. In particular, they are valid for any distance z from the source and for any range of real values $n(\omega)$ and $\alpha(\omega)$. It can be easily verified that $S(\mathbf{r}; \omega)$ reduces to $S^{(0)}(\omega)I(\boldsymbol{\rho})$ in the limit $z \to 0$, as one might expect. In the limit when $\alpha \to 0$, our formulation corresponds to the case of dispersive homogeneous media. The spectral modifier then becomes

$$M_h(\mathbf{r}; k; \omega) = \lim_{\alpha\to 0} M(\mathbf{r}; k, \alpha; \omega) = \frac{1}{z^2}\left(\frac{k\sigma_I}{\Delta_h}\right)^2 \exp\left[-\frac{k^2(x^2+y^2)/z^2}{2\Delta_h^2}\right], \tag{14}$$

where

$$\Delta_h = 2ab_h\sigma_I \tag{15}$$

and

$$b_h^2 = \frac{1}{2\sigma_I^2} + \left(\frac{k}{2az}\right)^2. \tag{16}$$

Equation (14) is also applicable to paraxial free-space propagation if we set $n(\omega) = 1$ so that $k = k_0$. Since spectral changes occurring on free-space propagation have attracted much attention, we consider this case first. We then consider the general case in which $n(\omega) > 1$ and $\alpha > 0$. In order to make our results readily available for experimental verification, we assume that the source spectrum $S^{(0)}(\omega)$ corresponds to that of a gallium phosphide (GaP) visible light source[40] and is well approximated by a Lorentzian line centered at 564 nm ($\nu_0 = \omega_0/2\pi \cong 532$ THz) with a FWHM of 36 nm ($\cong$34 THz). All the numerical results in this paper pertain to this source spectrum. The cross-spectral density of such a GaP source may not necessarily be of the form given by Eq. (8) on which our analysis is based. However, in practice, it is possible to modify it in such a way that it is approximates a Gaussian Schell-model source. The intensity distribution of GaP sources is often well approximated by a Gaussian function. The spatial correlation can be made Gaussian by passing the light through certain scatterers.[41–43] We assume that σ_I and σ_g are frequency independent for simplicity. However, our formulation is general enough to incorporate their frequency dependence when it is specified.

3. FREE-SPACE PROPAGATION

The changes in the spectrum of light on propagation through free space have been investigated extensively. However, a clear understanding of the spectral evolution with increasing propagation distance from the source is still lacking and may be due to the complexity of the computations involved.[4,44] Our analysis provides a relatively simple way for understanding the transition from near to far field within the paraxial approximation.[45]

In our notation the spectrum of the field after propagating a distance z in free space is given by

$$S_f(\mathbf{r}; \omega) = S^{(0)}(\omega)M_f(\mathbf{r}; \omega) = S^{(0)}(\omega)M_h(\mathbf{r}; k_0; \omega), \tag{17}$$

where M_f is the spectral modifier for free-space propagation that is obtained from M_h of Eq. (14) in the limit $k = k_0$. The far-zone behavior is obtained in the limit $k_0z \to \infty$ (with fixed direction of observation), and the spectrum of the field then reduces to

$$S_f^{(\infty)}(\mathbf{r}; \omega) = S^{(0)}(\omega)\left(\frac{k_0\sigma_I}{\sqrt{2}az}\right)^2 \exp\left[-\frac{k_0^2\sigma_I^2(x^2+y^2)/z^2}{4a^2}\right], \tag{18}$$

where the superscript (∞) indicates the far-zone limit. Equation (18) is in agreement, within the paraxial approximation, with a known result for far-zone radiant intensity of Gaussian Schell-model sources.[26]

We now return to the general expression for the spectrum of the field in free space [Eq. (17)] and evaluate the spectral modifier M_f for sources with different states of coherence governed by the values of σ_g and σ_I.

Figure 2 shows the variation of the spectral modifier M_f with the frequency ($\nu = \omega/2\pi$) for several choices of σ_g and σ_I when the propagation distance is $z = 1000\lambda_0/2\pi$ (i.e., $k_0z = 1000$), and the observation angle is 10° from the z axis. It follows from Eq. (17) that when the spectral modifier, considered as a function of ν, has a positive slope at $\nu = \nu_0$, the resulting line is blue shifted, whereas a negative slope of the spectral modifier at that frequency results in a red-shifted spectrum. If the spectral modifier is not uniform throughout the frequency range of the source spectrum, the nature of the spectral changes may be more complicated.[44] The examples shown in Fig. 2 correspond to a blue shift for $k_0\sigma_g <$

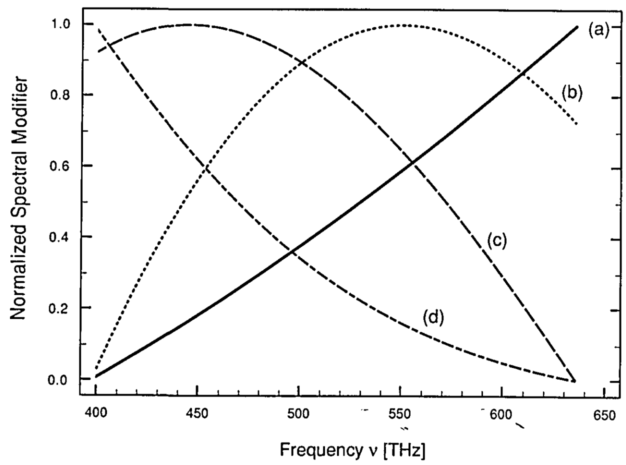

Fig. 2. Normalized spectral modifier M_f for propagation distance $k_0z = 100$ in free space. The spectral modifier is shown as a function of frequency ν for $k_0\sigma_I = 20$ and four different values of the correlation length: (a) $k_0\sigma_g = 1.0$, (b) $k_0\sigma_g = 8.0$, (c) $k_0\sigma_g = 10$, and (d) $k_0\sigma_g = 20$. The direction of the spectral shift is determined by the slope of M_f at the center frequency of the source.

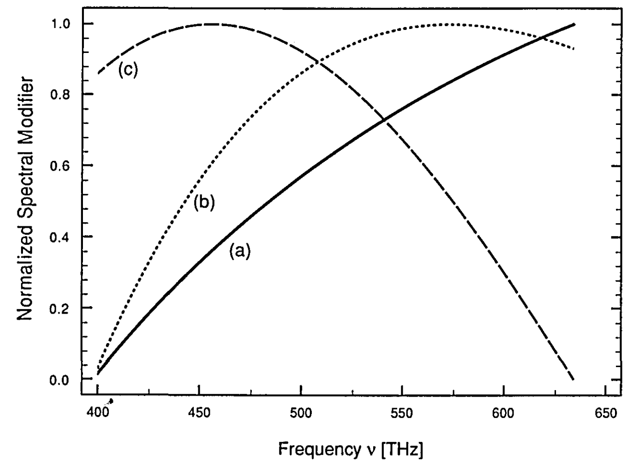

Fig. 3. Normalized spectral modifier M_f for three different propagation distances [(a) $k_0z = 100$, (b) $k_0z = 250$, and (c) $k_0z = 600$] in free space for $k_0\sigma_I = 20$, $k_0\sigma_g = 10$. At $\nu_0 = 532$ THz a blue shift is obtained for $k_0z = 100$ and a red shift for $k_0z = 600$.

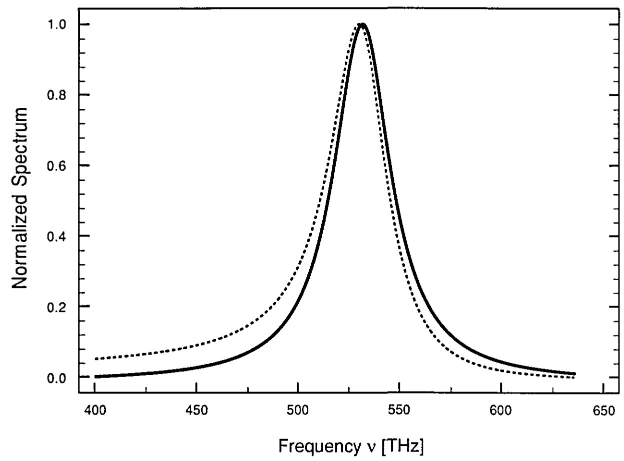

Fig. 4. Normalized field spectrum for observation at an angle of 10° off axis and a propagation distance $k_0z = 1000$. The source is characterized by $k_0\sigma_I = 20$ and $k_0\sigma_g = 20$. The solid curve shows the original source spectrum, and the dashed curve shows the red-shifted field spectrum.

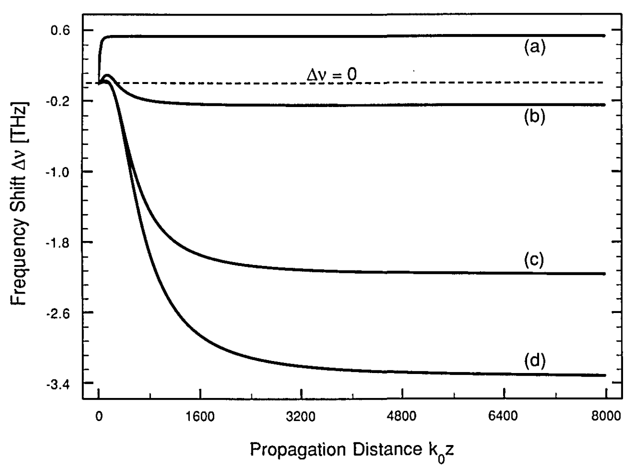

Fig. 5. Frequency shifts $\Delta\nu$ versus propagation distance for sources characterized by the same value of $k_0\sigma_I = 20$ and different values of $k_0\sigma_g$: (a) $k_0\sigma_g = 1$, (b) $k_0\sigma_g = 10$, (c) $k_0\sigma_g = 20$, (d) $k_0\sigma_g = 25$.

9 and a red shift for $k_0\sigma_g \geq 10$ for the GaP source for which $\nu_0 \cong 532$ THz.

For a given state of coherence, the spectral shift also depends on the propagation distance. This is shown in Fig. 3, where we compare the spectral modifier for different propagation distances when $k_0\sigma_I = 20$ and $k_0\sigma_g = 10$. We observe that the spectral shift would be toward higher frequencies for $k_0z = 100$ (positive slope at $\nu = \nu_0$) and toward lower frequencies for $k_0z = 600$ (negative slope at $\nu = \nu_0$). Figure 4 shows the spectra of the GaP source in the near zone ($k_0z = 10$) and in the far zone ($k_0z = 1000$) for $k_0\sigma_I = 20$ and $k_0\sigma_g = 20$. The source spectrum exhibits a red shift in the far zone and a slight blue shift that may be difficult to detect in the near zone. Note also that the spectrum becomes asymmetric as a result of propagation. These changes should be easy to observe experimentally.

We quantify the magnitude of the spectral shift by defining a parameter $\Delta\nu$ that corresponds to the shift of the spectral peak from the source spectrum. In Fig. 5 we show the spectral shift $\Delta\nu$ as a function of the propagation distance k_0z, for $k_0\sigma_I = 20$ and several values of $k_0\sigma_g$. We note that when the source is relatively incoherent ($k_0\sigma_g \leq 1$), the spectral shift, which is toward the blue for this angle of observation, develops rapidly with propagation distance. When the source is relatively coherent ($k_0\sigma_g \gg 1$), an initial blue shift turns into a red shift with increasing k_0z. For the states of coherence considered in this paper, the transition from the blue shift to red shift takes place for $k_0z \sim 100$. In all cases, the frequency shift becomes constant in the far zone. The constant value depends on $k_0\sigma_g$. The frequency shift for $k_0\sigma_g = 25$ [curve (d) in Fig. 5] is ~10% of the source spectral width (FWHM $\cong$ 34 THz).

4. HOMOGENEOUS MEDIA

We showed in Section 3 that the changes in the spectrum on propagation in free space depend on the state of coherence and on the propagation distance from the source. In this section we consider propagation through homogeneous media for which the index of refraction $n(\omega)$ differs from unity and is independent of position in space. It is, however, frequency dependent, a feature that indicates the dispersive nature of the homogeneous medium. The wave number is then given by

$$k = n(\omega)\,\frac{\omega}{c}. \tag{19}$$

On substituting Eq. (19) into Eqs. (14)–(16), we obtain the expression for the spectral modifier for dispersive homogeneous media. It sometimes happens that the refractive index $n(\omega)$ is nearly constant over the source spectral width. In that case, the medium acts as a nondispersive homogeneous medium of constant refractive index $n_0 = n(\omega_0)$, where ω_0 is the central frequency of the source spectrum. Let us consider the nondispersive case first.

It is evident from Eq. (14) that the spectral modifier M_h for a nondispersive homogeneous medium is identical to that of free space if k_0 is replaced by n_0k_0. Thus, the free-space results for the spectral modifier shown in Figs. 2 and 3 apply provided the scaling factor k_0 is appropriately modified. The spectral changes can be quite different as a result of the scaling. The comparison between the spectral changes occurring on propagation through free space and on propagation through homogeneous nondispersive media must be considered separately for distances short and long in comparison with a length $z_0 = k\sigma_I/\sqrt{2}a$ (obtained by requiring that the two terms in Eq. (16) contribute equally when $z = z_0$). For a short propagation range ($z \ll z_0$) the quantity k/Δ_h is independent of n_0; hence we expect no difference between the spectral changes occurring in dispersive homogeneous media and free space. For a long propagation distance ($z \gg z_0$), the quantity k/Δ_h appearing in Eq. (14) is larger by a factor $n(\omega)$ compared with free-space propagation. The extent of the spectral changes taking place under these circumstances depends on the value of n_0. In Fig. 6 we show a comparison of the spectral shifts for free space [curve (a)] and for two nondispersive homogeneous media with indices of refraction $n_0 = 1.5$ and $n_0 = 2$ [curves (b) and (c)] when $k_0\sigma_I = 20$ and $k_0\sigma_g = 10$. The most notable feature is that the far-zone value of the spectral shift increases with the increase in the refractive index n_0. This is an important feature. It shows that the Wolf effect is enhanced in a homogeneous medium.

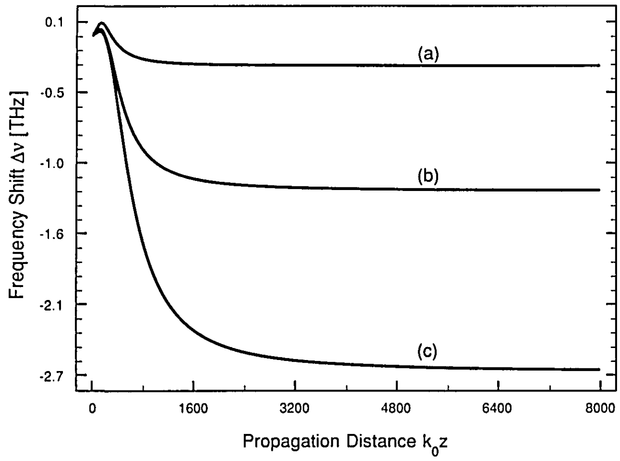

Fig. 6. Comparison of frequency shifts for propagation in nondispersive homogeneous media. The frequency shifts for a fixed angle of observation (10°) are shown for propagation in free space (a), for propagation in a homogeneous medium of an index of refraction n = 1.5 (b), and for propagation in a medium of index of refraction n = 2.0 (c). The observation angle is 10°, and the source parameters are $k_0\sigma_I = 20$ and $k_0\sigma_g = 10$.

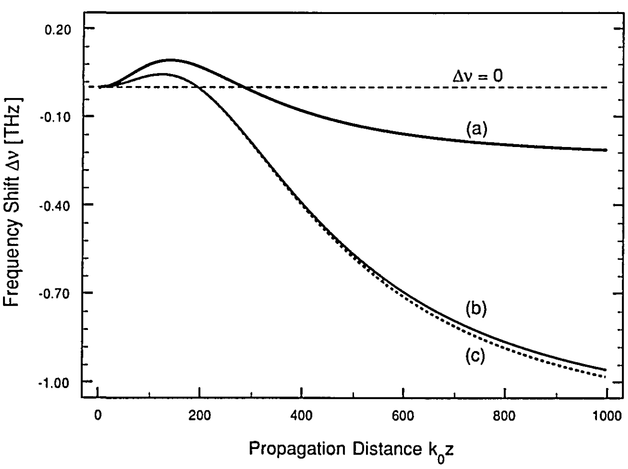

Fig. 7. Comparison of frequency shifts for dispersive homogeneous media. $\Delta\nu$ is shown as a function of k_0z for (a) propagation in free space, (b) propagation in pure silica, and (c) propagation in silica doped with 7.9% GeO_2. The observation angle is 10°, and the source parameters are $k_0\sigma_I = 20$ and $k_0\sigma_g = 10$.

We now consider the case of dispersive homogeneous media. As in the case of nondispersive media, we must consider the changes in the spectrum for short and long propagation distances separately. For a short propagation distance ($z \ll z_0$), the quantity k/Δ_h is again independent of the index of refraction, and the spectral effects are identical to those encountered on free-space propagation. For a long propagation distance ($z \gg z_0$), the quantity k/Δ_h depends on $n(\omega)$; as a result, the changes of the spectral effects in this medium from those generated in free space depend on the variation of $n(\omega)$ in the frequency range covered by the source spectrum. To consider a realistic case, we illustrate our results by using a slab of silica glass as an example of a dispersive homogeneous medium.

Figure 7 shows the frequency shift $\Delta\nu$ obtained after light from a GaP source propagates through a slab of silica glass of various thicknesses. The source parameters are $k_0\sigma_I = 20$ and $k_0\sigma_g = 10$. The frequency dependence of $n(\omega)$ was obtained by using the well-known Sellmeier equation[46]

$$n^2(\omega) = 1 + \sum_{j=1}^{3} \frac{B_j\omega_j^{\,2}}{\omega_j^{\,2} - \omega^2}. \tag{20}$$

For pure silica, the parameters are given by $B_1 = 0.696\,166\,3$, $B_2 = 0.407\,942\,6$, $B_3 = 0.897\,479\,4$, $\lambda_1 = 0.068\,404\,3$, $\lambda_2 = 0.116\,241\,4$, and $\lambda_3 = 9.896\,161$ μm, where $\lambda_j = 2\pi c/\omega_j$.

The effect of dopants on the spectral shift can be easily included in our analysis. For example, the refractive index $n(\omega)$ of silica glass can be increased by doping it with germania (GeO_2). The refractive index $n(\omega)$ is still given by the Sellmeier formula, but the parameters B_j and ω_j are different and depend on the amount of the dopant.[47] As an example, we consider silica glass doped with 7.9% GeO_2, for which the parameters are $B_1 = 0.713\,682\,4$, $B_2 = 0.425\,480\,7$, $B_3 = 0.896\,422\,6$, $\lambda_1 = 0.061\,716\,7$, $\lambda_2 = 0.127\,081\,4$, and $\lambda_3 = 9.896\,161$ μm. Figure 7 shows the expected change (dashed curve) in the frequency shift. The shift is slightly larger for doped silica since the dopant increases the refractive index by a small amount. In both cases (i.e., pure silica and slightly doped silica), the frequency shifts in the far zone are much larger than those that would be produced in free space.

The main conclusion of this section is that the Wolf effect is enhanced in a homogeneous medium of refractive index $n > 1$. The frequency dependence of the refractive index $n(\omega)$ is not critical for enhancement, since enhancement is found to occur even when n is frequency independent. The origin of the enhancement factor can be understood by referring to Eq. (14) and using $k = \omega n(\omega)/c$. The Gaussian factor in Eq. (14), plotted as a function of ω, is narrower for a homogeneous medium than for free space. It is this feature of the spectral modifier that is responsible for a larger spectral shift when $n > 1$.

5. INHOMOGENEOUS MEDIA

In this section we return to the general expression for the spectrum of light in a graded-index fiber [Eqs. (9)–(13)]. In this case the parameter α is nonzero; its value depends on the fiber design. We consider a specific fiber whose core is made of doped silica (7.9% GeO_2 at the core center) and a cladding made of pure SiO_2. For illustration, we use the same parameters for the core used in Section 4 for bulk silica. In practice, these parameters may be different for graded-index fibers, but such differences are easy to include in our formulation. If $n_1(\omega)$ is the refractive index at the core center ($\rho = 0$) and $n_2(\omega)$ is the refractive index at the boundary ($\rho = R_0$), the parameter α is given by

$$\alpha(\omega) = \frac{1}{R_0}\left[1 - \frac{n_2^{\,2}(\omega)}{n_1^{\,2}(\omega)}\right]^{1/2}. \tag{21}$$

Since $n_1(\omega)$ and $n_2(\omega)$ can be obtained by using Eq. (20), the frequency dependence of $\alpha(\omega)$ is readily determined. In the following calculations, the core radius is $R_0 = 25$ μm.

Figure 8 shows the frequency shift as a function of the propagation distance for $\alpha \neq 0$ [curve (a)] and compares it with those obtained for free space [curve (c)] and for a homogeneous medium of refractive index n_1 [curve (b)]. We

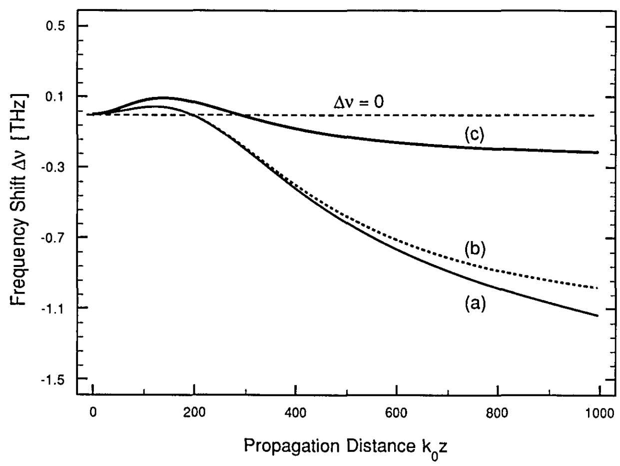

Fig. 8. Frequency shift $\Delta\nu$ versus the propagation distance k_0z in a dispersive graded-index medium [curve (a)]. Curve (b) shows $\Delta\nu$ when the inhomogeneous nature of the medium is ignored by setting $\alpha = 0$. Curve (c) shows, for comparison, the free-space result. The observation angle is 10°, and the source parameters are $k_0\sigma_I = 20$ and $k_0\sigma_g = 10$.

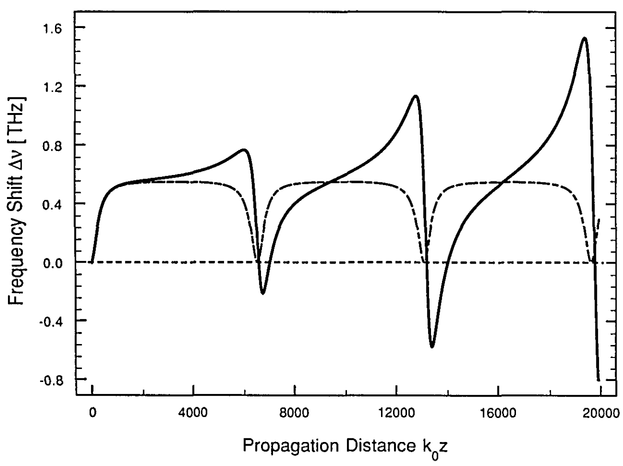

Fig. 9. Frequency shift $\Delta\nu$ as a function of propagation distance in a graded-index fiber (solid curve). The frequency shifts are calculated for observation at a fixed distance $10/k_0$ from the center of the fiber and $k_0\sigma_I = 20$ and $k_0\sigma_g = 10$. The dashed curve shows the frequency shifts when the frequency dependence of α is ignored by setting $[\alpha(\omega_0)/k_0 = 0.000\,48]$.

note that in the range of propagation distances shown in the figure, the frequency shift is larger for the graded-index medium compared with the homogeneous medium. This enhancement of the frequency shift is strictly due to the inhomogeneous nature of the medium and will clearly depend on the functional form of the inhomogeneity.

Although the frequency shift $\Delta\nu$ tends to a constant far-zone value in a homogeneous medium, no such limit exists in the graded-index medium considered here. This feature is due to the imaging property of a medium with a quadratic variation of the refractive index. Such a medium reproduces the incident field periodically with a period given by $z = 2\pi/\alpha$, a feature that is due to the periodic nature of the propagation kernel, Eq. (3). One would thus expect that the spectrum $S(\mathbf{r}; \omega)$ given by Eq. (5) also reduces to the source spectrum for $z = 2m\pi/\alpha$, where m is a positive integer. We show in Appendix B that this is indeed the case. Furthermore, we find that the source spectrum is reproduced not only at $z = 2m\pi/\alpha$, but also at $z = (2m + 1)\pi/\alpha$ except for a spatial inversion of the intensity distribution. For a symmetric intensity profile such as a Gaussian, $S(\mathbf{r}; \omega)$ is reproduced periodically with a period $z_p = \pi/\alpha$.

It would appear from the above discussion that the spectral shift should follow a periodic evolution pattern with the period z_p. However, this is not the case, as is evident from the solid curve in Fig. 9, where the spectral shift is plotted as a function of k_0z for propagation distances covering three periods ($k_0z_p \sim 6600$) for $k_0\sigma_I = 20$, $k_0\sigma_g = 10$, and α obtained by using Eq. (21). Figure 9 is drawn for a fixed radial distance from the fiber axis ($k_0(x^2 + y^2)^{1/2} = 10$) rather than for a fixed observation angle. This choice is made since the radial distance would exceed the fiber dimensions for such large propagation distances if the observation angle is kept fixed. Figure 9 shows that the frequency shift indeed becomes zero for $z_p = \pi/\alpha_0[\alpha_0 = \alpha(\omega_0)]$, but its maximum and minimum values become larger for successive periods.

The physical origin of the nonperiodic nature of the frequency shift can be traced back to the dispersive nature of the graded-index medium that makes α frequency dependent. Indeed, if α is replaced by α_0, we obtain the behavior indicated by the dashed curve in Fig. 9. It is clear from this curve that the frequency shift $\Delta\nu$ shows periodic behavior with period π/α_0 when the frequency dependence of α is ignored. When α is allowed to vary with frequency, $\Delta\nu$ becomes nonperiodic. We can understand this feature by noting that the period $z_p = \pi/\alpha$ itself becomes frequency dependent. Since the argument αz of the trigonometric functions appearing in Eqs. (11) and (13) is frequency dependent, we can expect z-dependent changes in the frequency shift. To conclude, the spectral shifts occurring in an inhomogeneous medium are strongly affected by the dispersive nature of the medium.

6. CONCLUSION

The changes in the spectrum of partially coherent light on propagation through homogeneous and inhomogeneous media were studied by using expressions derived for graded-index fibers. The results show, for the first time to our knowledge, the development of the spectral shift as a function of the propagation distance. They also show the dependence of the spectral shift on the index of refraction and the dispersion of the medium.

The development of the spectral shifts on propagation through an homogeneous medium depends on the spatial coherence of the source. When the source is relatively incoherent, the spectrum shifts toward the blue with increasing distance. On the other hand, when the spatial correlation is on the order of the source size, the spectrum develops a blue shift close to the source and gradually changes into a red shift with increasing propagation distance. The index of refraction and the dispersion of the medium are found to enhance the far-zone red shift. Our results for graded-index fibers show that the source spectrum is recovered periodically at distances at which such fibers image the source. The spectral shift, however, does not follow a strictly periodic pattern when the medium dispersion is taken into account.

We have presented our results by using the parameters corresponding to a common visible GaP source. Since graded-index fibers are also readily available, it should be possible to verify our theoretical predictions experimentally.

ACKNOWLEDGMENTS

The authors thank E. Wolf for helpful discussions concerning this manuscript. This research was supported by the New York State Science and Technology foundation and by the U.S. Army Research Office.

APPENDIX A: DERIVATION OF EQS. (9)-(13)

The spectrum of the field at any point $\mathbf{r}$ is given by

$$S(\mathbf{r};\omega)=\iint K^*(\mathbf{r},\rho_1;\omega)K(\mathbf{r},\rho_2;\omega)W(\rho_1,\rho_2;\omega)\mathrm{d}^2\rho_1\mathrm{d}^2\rho_2. \tag{A1}$$

Here $K(\mathbf{r}, \rho; \omega)$ is the propagator given by Eq. (2), and $W(\rho_1, \rho_2; \omega)$ is the cross-spectral density in the source plane given by Eq. (6). On substituting from Eq. (6) into Eq. (A1) we find that

$$S(\mathbf{r};\omega)=S^{(0)}(\omega)\left(\frac{k\alpha}{2\pi\sin\alpha z}\right)^2 I(x;\omega)I(y;\omega), \tag{A2}$$

where

$$I(x;\omega)=\iint \mathrm{d}\xi_1\mathrm{d}\xi_2\exp\left\{-\frac{\xi_2^2+\xi_1^2}{4\sigma_I^2}-\frac{(\xi_2-\xi_1)^2}{2\sigma_g^2}+\frac{ik\alpha}{\sin\alpha z}\left[\frac{\cos\alpha z}{2}(\xi_2^2-\xi_1^2)-x(\xi_2-\xi_1)\right]\right\}. \tag{A3}$$

To perform the two-dimensional integration we introduce the average and difference variables

$$\gamma_1=\tfrac{1}{2}(\xi_2+\xi_1), \tag{A4}$$

$$\gamma_1=\xi_2-\xi_1. \tag{A5}$$

Equation (A3) then takes the form

$$I(x;\omega)=\int \mathrm{d}\gamma_1\exp\left(-\frac{\gamma_1^2}{2\sigma_I^2}\right)\times\int \mathrm{d}\gamma_2\exp\left[-\gamma_2^2\left(\frac{1}{8\sigma_I^2}+\frac{1}{2\sigma_g^2}\right)+\frac{ik\alpha\gamma_2}{\sin\alpha z}(\gamma_1\cos\alpha z-x)\right]. \tag{A6}$$

If we define the parameter a by

$$a^2=\frac{1}{8\sigma_I^2}+\frac{1}{2\sigma_g^2}, \tag{A7}$$

and use the relation[48]

$$\int_{-\infty}^{\infty}\exp(-p^2x^2\pm qx)dx=\frac{\sqrt{\pi}}{p}\exp\left(\frac{q^2}{4p^2}\right), \tag{A8}$$

Eq. (A6) may be written as

$$I(x;\omega)=\frac{\sqrt{\pi}}{a}\exp\left[-x^2\left(\frac{k\alpha}{2a\sin\alpha z}\right)^2\right]\times\int \mathrm{d}\gamma_1\exp\left\{-\gamma_1^2\left[\frac{1}{2\sigma_I^2}+\left(\frac{k\alpha\cos\alpha z}{2a\sin\alpha z}\right)^2\right]\right\}\times\exp\left[2\gamma_1 x\cos\alpha z\left(\frac{k\alpha}{2a\sin\alpha z}\right)^2\right]. \tag{A9}$$

Next we define

$$b^2=\frac{1}{2\sigma_I^2}+\left(\frac{k\alpha\cos\alpha z}{2a\sin\alpha z}\right)^2 \tag{A10}$$

and use Eq. (A8) again to yield

$$I(x;\omega)=\frac{\pi}{ab}\exp\left\{-x^2\left(\frac{k\alpha}{2a\sin\alpha z}\right)^2\left[1-\left(\frac{k\alpha\cos\alpha z}{2ab\sin\alpha z}\right)^2\right]\right\}. \tag{A11}$$

We note that

$$\left[1-\left(\frac{k\alpha\cos\alpha z}{2ab\sin\alpha z}\right)^2\right]=\frac{1}{(2ab\sin\alpha z)^2}[(2ab\sin\alpha z)^2-(k\alpha\cos\alpha z)^2], \tag{A12}$$

which can be simplified, using Eq. (A10), to

$$\left[1-\left(\frac{k\alpha\cos\alpha z}{2ab\sin\alpha z}\right)^2\right]=\frac{1}{2b^2\sigma_I^2}. \tag{A13}$$

Substituting Eqs. (A11) and (A13) into Eq. (A2) and using a similar expression for $I(y; \omega)$, we obtain the expression

$$S(\mathbf{r};\omega)=S^{(0)}(\omega)\left(\frac{k\alpha}{2ab\sin\alpha z}\right)^2\times\exp\left[-(x^2+y^2)\frac{1}{2}\left(\frac{k\alpha}{2ab\sigma_I\sin\alpha z}\right)^2\right], \tag{A14}$$

which can be expressed in the form

$$S(\mathbf{r};\omega)=\frac{S^{(0)}(\omega)}{z^2}\left(\frac{k\sigma_I}{\Delta}\right)^2\exp\left[-\frac{k^2(x^2+y^2)/z^2}{2\Delta^2}\right], \tag{A15}$$

with

$$\Delta=2ab\sigma_I\frac{\sin\alpha z}{\alpha z}. \tag{A16}$$

APPENDIX B: PROOF OF THE PERIODIC REPRODUCTION OF THE SOURCE SPECTRUM

When the propagation distance satisfies the condition $\alpha z = m\pi$ for a positive integer m, some of the factors in Eq. (6) become singular. However, the spectrum of the field at such propagation distances remains well defined. In this appendix we use the method of stationary phase to evaluate the spectrum in the limit $z = m\pi/\alpha$. We start with Eq. (6) and rewrite it as

$$S(\mathbf{r};\omega)=\left(\frac{k\alpha\Lambda}{2\pi}\right)^2\iiiint \mathrm{d}\xi_1\mathrm{d}\xi_2\mathrm{d}\eta_1\mathrm{d}\eta_2 W(\xi_1,\xi_2,\eta_1,\eta_2;\omega)\times\exp\left\{ik\alpha\Lambda\left[\frac{\cos\alpha z}{2}(\xi_2^2-\xi_1^2+\eta_2^2-\eta_1^2)-x(\xi_2-\xi_1)-y(\eta_2-\eta_1)\right]\right\}, \tag{B1}$$

where Λ is defined by

$$\Lambda = \frac{1}{\sin \alpha z}. \tag{B2}$$

Since $\Lambda \rightarrow \infty$ as $z \rightarrow m\pi/\alpha$, we can evaluate the integral by using the method of stationary phase.[49] According to this method, if

$$I(\Lambda) \equiv \int f(t)\exp[i\Lambda\phi(t)]\mathrm{d}t, \tag{B3}$$

then

$$\lim_{\Lambda\rightarrow\infty} I(\Lambda) = \exp[i\Lambda\phi(d)]f(d)\left(\frac{2\pi}{\Lambda|\phi''(d)|}\right)^{1/2} \times \exp\left(\frac{i\pi\mu}{4}\right) + O(\Lambda^{-3/2}). \tag{B4}$$

Here d is a zero of ϕ' and $\mu = \mathrm{sgn}[\phi''(d)]$.[50] Applying this formalism to Eq. (B1) with the definitions

$$\phi(\xi_2) = k\alpha\left(\frac{\cos \alpha z}{2}\xi_2^{\,2} - x\xi_2\right), \tag{B5}$$

and

$$f(\xi_2) = W(\xi_1, \xi_2, \eta_1, \eta_2), \tag{B6}$$

we find that

$$I(\Lambda) = \left(\frac{2\pi}{\Lambda k\alpha}\right)^{1/2} \exp\left(\frac{i\pi\mu}{4}\right)\exp\left[\frac{ik\alpha}{\cos \alpha z}x^2\left(\frac{1}{2} - \frac{1}{\cos \alpha z}\right)\right] \times W\left(\xi_1, \frac{x}{\cos \alpha z}, \eta_1, \eta_2\right) + O(\Lambda^{-3/2}). \tag{B7}$$

We repeat the same procedure for the integration over the variables ξ_1, η_1, and η_2 and take the limit $\Lambda \rightarrow \infty$. All the phase factors cancel, and the final result is

$$S(\mathbf{r}; \omega) = W\left(\frac{x}{\cos \alpha z}, \frac{x}{\cos \alpha z}, \frac{y}{\cos \alpha z}, \frac{y}{\cos \alpha z}; \omega\right). \tag{B8}$$

Since $\cos \alpha z = \pm 1$, we see from Eq. (B8) that the spectrum of the source is completely reproduced at propagation distances $z = 2m\pi/\alpha$, whereas for propagation distances $z = (2m + 1)\pi/\alpha$ the spectrum of the source is again reproduced, aside from spatial inversion. For a symmetric intensity profile such as a Gaussian, the source spectrum and the intensity distribution are both reproduced at $z = m\pi/\alpha$. We emphasize that Eq. (B8) is exact at $z = m\pi/\alpha$ in spite of our use of the method of stationary phase for evaluating the integrals in Eq. (B1).

REFERENCES AND NOTES

1. E. Wolf, "Non-cosmological redshifts of spectral lines," Nature (London) **326**, 363–365 (1987).
2. E. Wolf, "Redshifts and blueshifts of spectral lines caused by source correlations," Opt. Commun. **62**, 12–16 (1987).
3. E. Wolf, "Red shifts and blue shifts of spectral lines emitted by two correlated sources," Phys. Rev. Lett. **58**, 2646–2648 (1987).
4. Z. Dacic and E. Wolf, "Changes in the spectrum of a partially coherent light beam propagating in free space," J. Opt. Soc. Am. A **5**, 1118–1126 (1988).
5. A. Gamliel, "Spectral changes in light propagation from a class of partially coherent sources," in *Proceedings of 6th Rochester Conference on Coherence and Quantum Optics (1989)*, J. H. Eberly, L. Mandel, and E. Wolf, eds. (Plenum, New York, 1990).
6. E. Wolf, "Invariance of spectrum of light on propagation," Phys. Rev. Lett. **56**, 1370–1372 (1986).
7. A. Gamliel and E. Wolf, "Spectral modulation by control of source correlations," Opt. Commun. **65**, 91–96 (1988).
8. J. T. Foley and E. Wolf, "Partially coherent sources that generate the same far-field spectra as completely incoherent sources," J. Opt. Soc. Am. A **5**, 1683–1687 (1988).
9. D. F. V. James and E. Wolf, "A spectral equivalence theorem," Opt. Commun. **72**, 1–6 (1989).
10. J. T. Foley, "The effect of an aperture on the spectrum of partially coherent light," Opt. Commun. **75**, 347–352 (1990).
11. G. M. Morris and D. Faklis, "Effects of source correlations on the spectrum of light," Opt. Commun. **62**, 5–11 (1987).
12. M. F. Bocko, D. H. Douglass, and R. S. Knox, "Observation of frequency shifts of spectral lines due to source correlations," Phys. Rev. Lett. **58**, 2649–2651 (1987).
13. F. Gori, G. Guattari, C. Palma, and G. Padovani, "Observation of optical redshifts and blueshifts produced by source correlations," Opt. Commun. **67**, 1–4 (1988).
14. D. Faklis and G. M. Morris, "Spectral shifts produced by source correlations," Opt. Lett. **13**, 4–6 (1988).
15. G. Indebetouw, "Synthesis of polychromatic light sources with arbitrary degrees of coherence: some experiments," J. Mod. Opt. **36**, 251–259 (1989).
16. H. C. Kandpal, J. S. Vaishya, and K. C. Joshi, "Wolf shift and its applications in spectroradiometry," Opt. Commun. **73**, 173–178 (1989).
17. Statements about the variance of the spectrum are also found in L. Mandel, "Concept of cross-spectral purity in coherence theory," J. Opt. Soc. Am. **51**, 1342–1350 (1961).
18. F. Gori and R. Grela, "Shape invariant propagation of polychromatic fields," Opt. Commun. **49**, 173–177 (1984).
19. A. Ghatak and K. Thyagarajan, "Graded index optical waveguides: a review," in *Progress In Optics XVIII*, E. Wolf, ed. (North-Holland, Amsterdam, 1980), pp. 1–126.
20. G. P. Agrawal, A. K. Ghatak, and C. L. Metha, "Propagation of a partially coherent beam through Selfoc fibers," Opt. Commun. **12**, 333–337 (1974).
21. P. Spano, "Connection between spatial coherence and modal structure in optical fibers and semiconductor lasers," Opt. Commun. **33**, 265–270 (1980).
22. S. Piazzola and P. Spano, "Spatial coherence in incoherently excited optical fibers," Opt. Commun. **43**, 175–179 (1982).
23. M. Imai and Y. Ohtsuka, "The influence of mode-coupling on the degree of coherence in an optical fiber," Opt. Commun. **45**, 331–335 (1983).
24. M. Imai, S. Satoh, and Y. Ohtsuka, "Complex degree of spatial coherence in an optical fiber: theory and experiment," J. Opt. Soc. Am. A **3**, 86–93 (1986).
25. M. Born and E. Wolf, *Principles of Optics*, 6th ed. (Pergamon, New York, 1983), Sec. 10.3.
26. See, for example, E. Wolf and E. Collett, "Partially coherent sources which produce the same far-field intensity distribution as a laser," Opt. Commun. **25**, 293–296 (1978).
27. D. Marcuse, *Light Transmission Optics* (Van Nostrand Reinhold, New York, 1972), p. 267.
28. See also E. Wolf, "New theory of partial coherence in space-frequency domain. Part I: Spectra and cross-spectra of steady-state sources," J. Opt. Soc. Am. **72**, 343–351 (1982); "Part II: Steady-state fields and higher-order correlations," J. Opt. Soc. Am. A **3**, 76–85 (1986).
29. A. C. Schell, "A technique for the determination of the radiation pattern of a partially coherent aperture," IEEE Trans. Antennas Propag. **AP-15**, 187–188 (1967).
30. A. T. Friberg and J. Turunen, "Imaging of Gaussian Schell-model sources," J. Opt. Soc. Am. A **5**, 713–720 (1988).
31. A. T. Friberg and R. J. Sudol, "The spatial coherence properties of Gaussian Schell-model beams," Opt. Acta **30**, 1075–1097 (1983).
32. A. Gamliel, "Radiation efficiency of planar Gaussian Schell-model sources," Opt. Commun. **60**, 333–338 (1986).
33. P. De-Santis, F. Gori, G. Guattari, and C. Palma, "Anisotropic Gaussian Schell-model sources," Opt. Acta **33**, 315–326 (1986).
34. R. Simon, E. C. G. Sudarshan, and N. Mukunda, "Anisotropic Gaussian Schell-model beams: passage through optical systems and associated invariants," Phys. Rev. A **31**, 2419–2434 (1985).

35. J. Deschamps, D. Courjon, and J. Bulabois, "Gaussian Schell-model sources: an example and some perspectives," J. Opt. Soc. Am. **73,** 256–261 (1983).
36. A. Starikov and E. Wolf, "Coherent-mode representation of Gaussian Schell-model sources and of their radiation fields," J. Opt. Soc. Am. **72,** 923–928 (1982).
37. Li Yajun and E. Wolf, "Radiation from anisotropic Gaussian Schell-model sources," Opt. Lett. **7,** 256–258 (1982).
38. A. T. Friberg and R. J. Sudol, "Propagation parameters of Gaussian Schell-model beams," Opt. Commun. **41,** 383–387 (1982).
39. J. T. Foley and M. S. Zubairy, "The directionality of Gaussian Schell-model beams," Opt. Commun. **26,** 297–300 (1978).
40. See, for example, Texas Instruments type TIL211, Bulletin No. DS-S 7412095, March 1974.
41. F. Scudieri, M. Bertolotti, and R. Bartolino, "Light scattered by a liquid crystal: a new quasi-thermal source," Appl. Opt. **13,** 181–185 (1974).
42. P. de Santes, F. Gori, G. Guattari, and C. Palma, "An example of a Collett–Wolf source," Opt. Commun. **29,** 256–260 (1979).
43. J. D. Farina, L. M. Narducci, and E. Collett, "Generation of highly directional beams from a globally incoherent source," Opt. Commun. **32,** 203–208 (1980).
44. A. Gamliel, "Mode analysis of spectral changes in light propagation from sources of any state of coherence," J. Opt. Soc. Am. A **7,** 1591–1597 (1990).
45. G. P. Agrawal and A. Gamliel, "Spectrum of partially coherent light: transition from near to far zone," Opt. Commun. **78,** 1–6 (1990).
46. G. P. Agrawal, *Nonlinear Fiber Optics* (Academic, New York, 1989), pp. 7–8.
47. The calculations appearing in this paper were based on M. J. Adams, *An Introduction to Optical Waveguides* (Wiley, New York, 1981), pp. 244–245.
48. I. S. Gradshteyn and I. M. Ryzhik, *Table of Integrals, Series, and Products* (Academic, New York, 1980), Sec. 3.323.2.
49. N. Bleistein and R. A. Handelsman, *Asymptotic Expansions of Integrals* (Holt, Rinehart & Winston, New York, 1975), Chap. 6.
50. In general there may be more than one zero of ϕ'. In the case that we are considering there is a single zero and hence Eq. (B4) does not contain the usual summation over all the roots of the equation $\phi' = 0$.